ACS Sustainable Chemistry & Engineering

pubs.acs.org/journal/ascecg

Research Article

Ultralow-Cost Hydrogel Electrolytes Based on Agricultural Byproducts for Distributed Electrophysiological Recording in Resource-Limited Settings

Lilian C. Alarcón-Segovia,[♦] Kenneth E. Madsen,[♦] Claire Liu, Sun Hong Kim, Tae Wan Park, Yayun Du, Joanna L. Ciatti, Kathrin H. Salame, Jae-Young Yoo, and John A. Rogers*

Cite This: *ACS Sustainable Chem. Eng.* 2025, 13, 6051−6063

Read Online

ACCESS | Metrics & More | Article Recommendations | Supporting Information

ABSTRACT: Global access to quality healthcare remains one of the most pressing issues for modern society. Despite advances in wearable and point-of-care biomedical devices, the dissemination of these technologies to resource-limited populations remains challenging, partially due to limitations imposed by cost. One of the largest cost drivers in the adoption of wearable devices for electrophysiological (ExG) monitoring, for instance, is the consumable overhead (electrolytes, adhesives, and electrodes) necessary to support patient use. Herein, we report the development and optimization of ultralow-cost (<0.03 USD per electrode), stable, and resource-available ExG electrolytes fabricated from agricultural byproducts widely available in local settings, thereby negating the dependency on importation. We show that composite hydrogels can be prepared from a variety of starch precursors via a facile one-pot sol−gel method to yield ionically conductive, mechanically compliant gel electrolytes. We further demonstrate that food starch materials for these purposes are resistant to dehydration and, when coupled with a wireless recording platform, can facilitate long-term (8 h) signal recording without significant loss in signal quality. Together, these characteristics mark starch-based electrolytes as possible alternatives to commercial formulations for skin-interfaced measurement electrodes, compatible with mobile sensing apparatus in resource-limited settings with cost, sustainability, and supply chain advantages without sacrificing clinical performance.

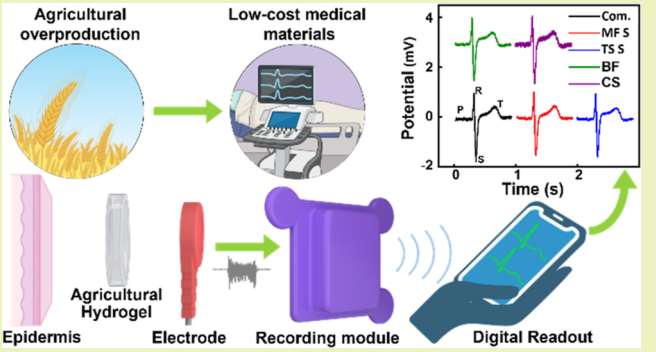

KEYWORDS: *hydrogel, electrophysiology, low-cost, agricultural waste, distributed healthcare*

INTRODUCTION

Recent technological advances in diagnostic and therapeutic medical devices can now support continuous data collection in point-of-care settings.[1−3] The proliferation of these platforms is readily apparent from both the commercial success and academic interest in wearable "smart," health devices including watches,[4,5] rings,[6,7] gloves,[8,9] glasses,[10−12] and dermal patches.[13−16] These devices are effective at tracking physiological characteristics during daily activity (heart rate, heart rate variability, skin temperature, movement/activity, etc.), and their adoption as diagnostic tools for digital medicine is growing.[17] At present, however, the high cost of commercially available wearable medical devices largely precludes their deployment in resource-limited settings, where the benefits of such technologies could be transformative. Pursuant the global distribution of high-quality healthcare, the development of clinical grade, low-cost biomedical devices remains an outstanding challenge.[18]

Currently, one of the most mature application areas for wearable devices is electrophysiological (ExG) monitoring including electrocardiography (ECG), electromyography (EMG), and electroencephalography (EEG). These methods, collectively regarded as ExG, remain among the most powerful techniques in diagnostic medicine, making their widespread dissemination a benefit for healthcare providers. Currently, wearable devices for such purposes are already the standard of care for outpatient cardiac arrythmia diagnosis in high-income countries, representing an $8 billion USD market with the expectation to double in size by 2030.[19] Unfortunately, despite significant research effort in the development of wearable/wireless ExG platforms,[20−22] comparatively little attention has been devoted to the consumable materials necessary to support them. Notably, the cost and availability of electrolyte gels,

Received: September 22, 2024
Revised: April 14, 2025
Accepted: April 15, 2025
Published: April 21, 2025

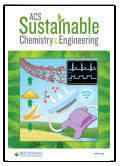

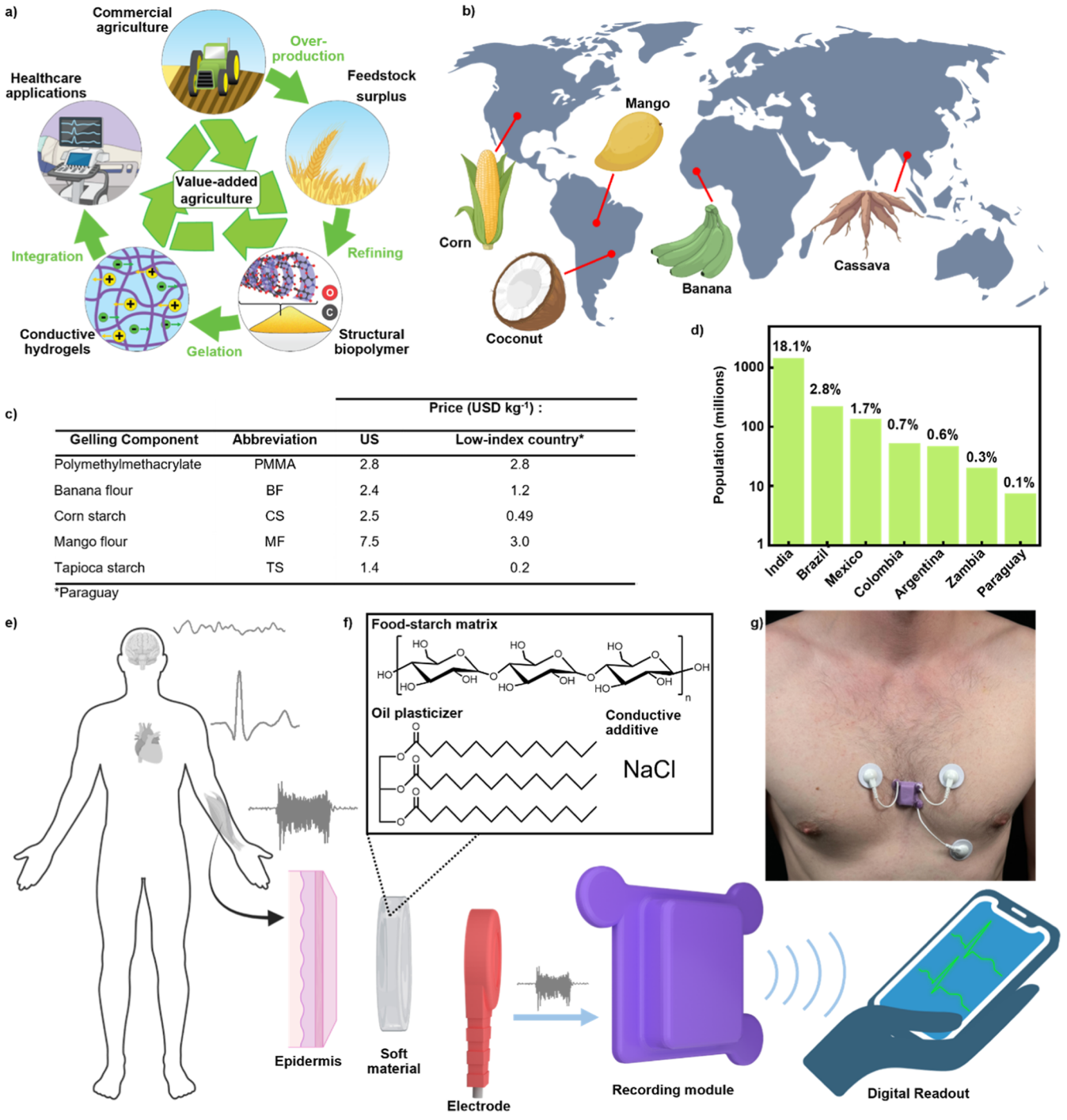

Figure 1. (a) Application pipeline for the use of agricultural byproducts in clinical biomedical technologies. (b) Commonly overproduced sources of food starch separated by geographic region. (c) Bulk cost of agricultural feedstocks in the United States and in a low-HDI country (Paraguay). (d) Populations affected by limited access to widespread healthcare services. (e) Schematic depiction of ExG signal collection using a hydrogel electrolyte connected via an electrode to a wireless data acquisition and transmission system. (f) General composition of food starch hydrogel electrolytes. (g) Photograph depicting a wireless recording module adhered to the chest for continuous ECG collection. (a,b,e) Use assets obtained from BioRender.com.

adhesives, and associated electrode materials must be carefully considered to ensure the successful global deployment of ExG devices, particularly in resource-constrained areas where the need is greatest.[23] Also, from a sustainability perspective, the healthcare industry already represents a substantial contributor to greenhouse emissions and solid waste streams, with 85% of medical waste composed of plastic packaging, single-use tools, and diagnostic devices.[24] While recent reports have demonstrated reusable electrodes/electrolytes for EXG recording,[25−27] an alternative approach exists leveraging local precursor materials to produce electrode assemblies on demand at low cost. Herein, we explore this approach through the development of stable, highly conductive hydrogel electrolytes fabricated from low cost and locally available agricultural byproducts in the form of food starches, as displayed conceptually in Figure 1a.

https://doi.org/10.1021/acssuschemeng.4c07823
ACS Sustainable Chem. Eng. 2025, 13, 6051−6063

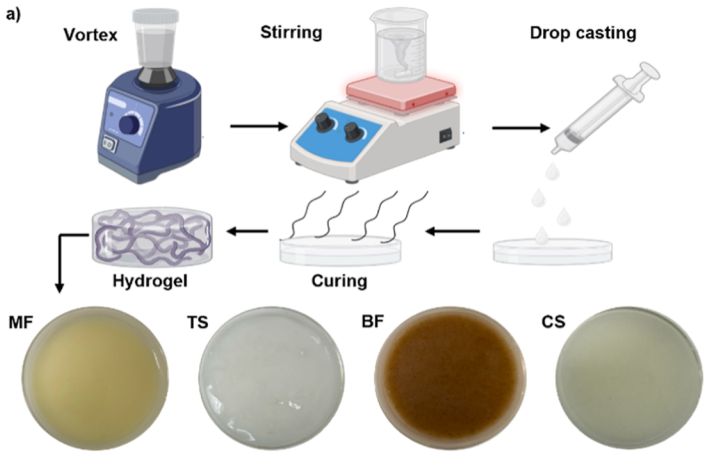

b)

Sample Designation	Sample Composition	Starch (wt. %)	Oil (wt. %)	Glycerol (wt. %)	NaCl (wt. %)
MF	Mango flour base composition	10	2	--	1
MF O	Increased plasticizer loading	10	5	--	1
MF S	Increased NaCl loading	10	2	--	2
TS	Tapioca starch base composition	10	2	--	1
TS O	Increased plasticizer loading	10	5	--	1
TS S	Increased NaCl loading	10	2	--	2
CS	Corn starch base composition	9	--	9	2
BF	Banana flour base composition	9	--	9	2

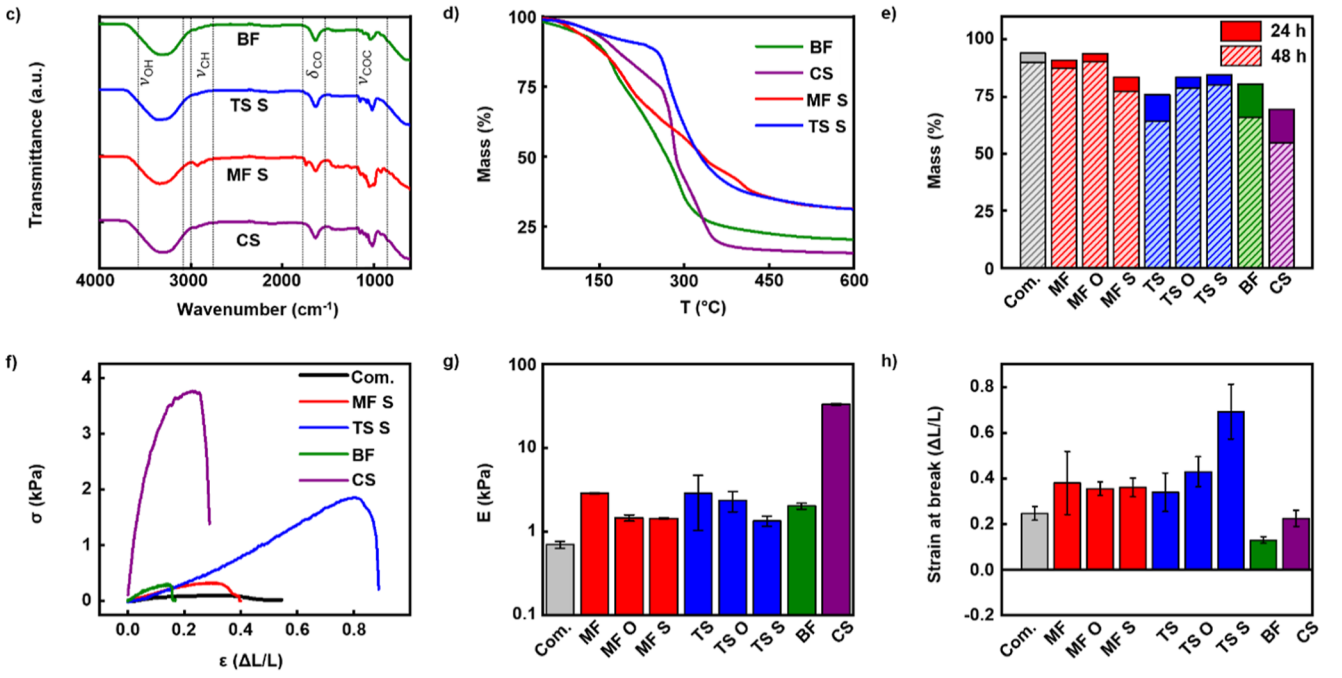

Figure 2. (a) Fabrication approach for starch-based hydrogel electrodes and photographs of the resulting gel materials. (b) Hydrogel compositions and designations (c) FTIR collected from as-prepared hydrogel samples. (d) Thermogravimetric analysis of as-prepared hydrogels. (e) Evaporative mass loss from hydrogel electrolytes during storage in a dry environment. (f) Dynamic mechanical analysis of hydrogel electrolytes. (g) Young's moduli obtained from hydrogel electrolytes. (h) Breaking strain obtained from hydrogel electrolytes. (a) Uses assets obtained from BioRender.com.

Chemically, starches represent an interesting, and underexplored, class of structural polymers owing to the high chemical stability and structural variety of naturally produced polysaccharide networks.[28,29] The prevalence of linear (helical amylose) and branched (amylopectin) polysaccharides promotes the formation of stable gel composites from hydrated starches.[30−33] Additionally, agricultural overproduction of starch foodstuffs is a common occurrence in rural areas, such that starch-rich feedstocks are often discarded as agricultural byproducts.[34,35] While their utilization in ExG applications remains limited, recent work demonstrates the potential of these byproducts to serve as structural components for ecofriendly, nontoxic, and even edible forms of simple electronic components, making their deployment as constituent materials in bioelectronic applications a distinct possibility.[36−38]

In addition to the chemical and structural properties of starch-based biopolymers, the geographic distribution of starchy foodstuffs makes them a readily available global resource, as displayed in Figure 1b. In conjunction with this geographic availability, the bulk price of agricultural starches is equivalent to or lower than that of conventional polymers [poly(methyl methacrylate), PMMA] used in the fabrication of commercial ExG electrolytes.[39] Figure 1c presents the bulk prices of various food starches from vendors based in the United States and in Paraguay, highlighting the potentially significant cost reductions associated with the use of food starch hydrogel electrolytes for ExG recording. Similarly, the high availability of local starch feedstocks could provide a significant benefit to populations that have limited access to chemical suppliers, including rapidly increasing populations in Mexico, Colombia, Brazil, Paraguay, Argentina, Zambia, and India, which, taken together, represent over 20% of the global population, as displayed in Figure 1d.

Herein, we present the fabrication and optimization of hydrogel electrolytes assembled from a diverse collection of readily available food starches via a facile sol−gel method using

https://doi.org/10.1021/acssuschemeng.4c07823
ACS Sustainable Chem. Eng. 2025, 13, 6051−6063

NaCl and lipophilic plasticizers (oil or glycerol) to improve the ionic conductivity and mechanical compliance, respectively (Figure 1f). We demonstrate clinical-quality ExG recording using starch-based electrodes at a price point of 0.025 USD per electrode. Likewise, we validate the deployability of these hydrogel electrolytes in a real-world setting, using a wearable, wireless recording module to realize long-term (8 h) continuous ECG recording based on the schematic protocol depicted in Figure 1e. Overall, coupling these low-cost hydrogel electrolytes with a portable, versatile, and reusable wearable platform (Figure 1g) to record high-quality biopotential data could prove significant in the widespread distribution of quality healthcare in low human development index (HDI) settings.

MATERIALS AND METHODS

Materials. Unless otherwise stated, all materials were used as received without further purification. Conductive hydrogels were assembled from the following food-grade starches: mango powder (Koyah, USA), tapioca starch (Goya, USA), corn starch (Maizena, Mx), and banana flour (livekuna, USA). Gels were plasticized with glycerol (87%, Sigma-Aldrich) and fractionated coconut oil (Handcraft Blends, USA) using NaCl (99%, Sigma-Aldrich, USA) as a conductive additive. Milli-Q water (18.2 MΩ resistivity) was used as the solvent for all sample preparations. Electrode assemblies were fabricated from foam sheets (EVA foam, 1 mm thick, Do^{2}ping, USA), flat snap Ag/AgCl electrodes (TDE-202, Florida Research Instruments, USA), and double-sided medical adhesive (1509, 3M, USA). Alcohol preparatory pads (Dealmed, USA) and skin preparation gel (NUPREP, Balego, USA) were used to sanitize and prepare skin for ExG recording. Commercially available recording electrodes (2560-5, 3M, USA) were used to compare the performance of food-based hydrogels to the current clinical standard.

Hydrogel Electrode Preparation. Food-based gel electrolytes were prepared via a modified sol−gel method[40,41] as depicted schematically in Figure 2a. Briefly, an aqueous solution of the forming polymer (food starch), conductive additive (NaCl), and plasticizer was prepared and coarsely homogenized with a vortex mixer (1 min, Vortex-Genie 2, Scientific Industries Inc., USA) to break down individual starch granules and to encourage water infiltration into the powdered starch. This solution was then heated to 170 °C for 30 min under constant stirring (450 rpm) to affect the uncoiling of individual amylose and amylopectin chains to form a robust gel network.[42] The resulting precursor solution was then poured into a polycarbonate Petri dish to an approximate thickness of 3 mm and allowed to cure at 40 °C for 4 h (Figure S1 provides viscosities for different precursor solutions). After curing, the completed hydrogel was punched into circular electrodes (15 mm diameter) using an arch punch and stored in a hermetically sealed container until the time of measurement. The mass compositions of hydrogels considered here were varied according to Figure 2b to study the mechanical and electrical characteristics accessible to this class of starch-based electrolyte (highlighted rows represent the optimized compositions used for subsequent ExG studies). For each composition, the addition of a compatible plasticizing agent was necessary to avoid gel tearing during curing. While gels based on tapioca starch and mango flour formed stable homogeneous mixtures using fractionated coconut oil as a plasticizing agent, gels based on banana flour and corn starch displayed phase separation during curing, resulting in an inhomogeneous mixture. To address this issue, banana and corn starches were plasticized with glycerol, which demonstrated greater compatibility during curing. NaCl was also added to improve the ionic conductivity of the gel composites.

Hydrogel punches were used to assemble functional electrodes for physiological recording as follows: foam rings (15 mm inner diameter, 50 mm outer diameter, and 1 mm thickness) were laser cut (VLS 3.60DT, Universal Laser Systems, USA) and used to define the size of the hydrogel/skin interface. A layer of double-sided medical adhesive was then cut to the same dimensions as the foam support and attached to the skin-facing side of the assembly. An Ag/AgCl snap electrode was then placed in the center of the foam ring and adhered to the structure with a layer of single-sided adhesive. A hydrogel punch was then placed in contact with the Ag/AgCl surface to finalize the assembly as depicted schematically in Figure S2. This structure provided a stable support for hydrogel electrodes and a favorable adhesive interface between the electrode and the skin. The total cost of each of these electrodes was less than 0.03 USD, determined from the price of bulk raw materials (see Table S1 for a detailed cost analysis).

Chemical and Structural Analysis. Hydrogel samples were initially characterized by using Fourier transform infrared spectroscopy with an attenuated total reflectance module (FTIR-8201 PC, Shimadzu, Tokyo, Japan) to identify functional groups contributing to the electrical and mechanical properties of the composite. Surface topologies were obtained by optical profilometry with a digital light microscope (VHX-XF, Keyence, USA) and used to compute the root-mean-square surface roughness of the as-prepared hydrogel samples. Thermogravimetric analysis was performed within a temperature window of 25−600 °C at a heating rate of 10 °C min^{-1} under a flowing nitrogen atmosphere (90 sccm) using a thermobalance (Q500, TA Instruments, USA). Room temperature evaporative mass loss was characterized with an analytical balance (Brand, USA) by sequentially measuring the mass of hydrogel samples during long-term storage in a low-humidity environment (a sealed desiccator with a $Ca(SO_4)_2$ desiccant, Drierite, USA). The viscosity of hydrogel precursor solutions was measured in air using a rheometer (MCR 302, Anton Paar, USA) under a constantly increasing temperature. Temperature was ramped at a constant rate of 1 °C min^{-1} from 25 to 30 °C. The biodegradability of hydrogel electrolytes was evaluated with accelerated aging tests wherein circular electrolyte samples (1 cm diameter) were soaked in 10 mL of phosphate-buffered saline at 50 °C. Digital photographs were collected at 24 h intervals to evaluate the hydrolytic decomposition of each gel composite. Scanning electron microscopy of Ag/AgCl electrodes prior to and after 48 h contact with hydrogel electrolytes was performed using an FEI Quanta 650 microscope at an accelerating voltage of 30 kV.

Mechanical Characterization. The stress−strain characteristics, Young's modulus, and elongation at break of representative hydrogel samples were obtained using a motorized force tester (Mark-10, USA) equipped with a 10 N load cell. All tests were performed at room temperature with rectangular samples measuring 22 mm in length and 7 mm in width. Samples were stretched until they broke at a constant rate of 10 mm min^{-1}. The engineering stress was computed by normalizing the total stress by the cross-sectional area of the sample (the product of the sample's width and thickness). Young's moduli were calculated by differentiation of the linear domain of the resulting stress−strain curves. Skin adhesion measurements were conducted on the forearms of healthy human subjects by affixing 1 cm diameter gel samples to the motorized stage and advancing them until they formed compressive contact with the skin. The gels were then retracted at a constant rate of 10 mm min^{-1} to evaluate the force necessary to detach them from the skin.

Electrochemical Characterization. The ionic conductivity and charge transfer characteristics of hydrogel electrolytes were determined with potentiometric electrochemical impedance spectroscopy (EIS) using a benchtop potentiostat (PGSTAT 128N, Metrohm Autolab, The Netherlands). Circular hydrogel punches (15 mm diameter) were placed between two identical Ag/AgCl electrodes, across which a sinusoidal voltage perturbation was applied (25 mV amplitude). Samples were characterized within a frequency window of 1 Hz to 10 kHz to capture charge transfer dynamics at the AgCl/hydrogel interface and ion mobility in the bulk hydrogel. Impedance spectra were analyzed computationally by fitting experimental data to a modified Randle's circuit (ZFit software, Biologic, France). Due to the high ionic conductivity of the gel, and the close spacing of the electrodes (between 2 and 6 mm), a finite diffusion element was used to consider bulk ion conductivity in lieu of the more traditional semi-infinite Warburg element as described elsewhere.[43]

https://doi.org/10.1021/acssuschemeng.4c07823
ACS Sustainable Chem. Eng. 2025, 13, 6051−6063

Contact impedance was characterized using EIS (25 mV amplitude, 0.1 to 10^5 Hz frequency range) with commercial PMMA-based electrodes serving as counter and reference electrodes, respectively. A three-electrode assembly was applied to the forearms of healthy human subjects with electrodes placed 5 cm apart. Measurements were repeated at 24 and 48 h intervals of dry storage. Spectra were fit using a simplified RC equivalent circuit as described elsewhere.[44]

Wireless Electrophysiology Recording Device. The wireless recording device considered here consisted of a clinical grade ECG chipset (MAX30003, Analog Devices, USA) to facilitate data acquisition and a Bluetooth low energy (BLE) system on a chip (SoC, ISP-1807, Insight SIP) to accommodate data transmission. A 4-GB flash memory (MT29F4G01ABAFDWB-IT:F, Micron) was also implemented to account for interruptions in the BLE communication. All chips were integrated into a flexible printed circuit board and subsequently encapsulated with a silicon elastomer (Sylgard 184, Dow, USA). The sampling rate of the recording system was fixed at 250 Hz.

Adhesive-Free Electrode Harness. A soft, conformable electrode harness was fabricated from low-cost materials to demonstrate the feasibility of an adhesive-free EXG recording with starch-based hydrogel electrolytes. EVA foam (10 mm thick, Do^{2}ping, USA) was cut by hand using the stenciled designs provided in Figure S3 to form the body of the harness. Layers of foam were adhered together using a hot glue gun (Surebonder, USA) with aluminum armature wire (16 gauge, Richeson, USA) placed between layers to provide structural rigidity and adjustability. Braided elastic bands (Dritz, USA) were used in conjunction with hook and loop fabric (Velcro, USA) to provide elastic contact between the skin and the harness. Finally, the wireless recording device described above was connected to snap electrodes via jumper wires and held in place with a foam cover to complete the assembly.

Human Subject Testing. ExG studies were performed on healthy consenting adults and were approved by the Northwestern University Institutional Review Board, Chicago, IL, USA (STU00221965). Prior to measurement, the participants' skin was sanitized with an alcohol preparatory pad, and the surface layer of the epidermis was removed using NUPREP gel. Following skin preparation, electrodes were adhered to the skin and connected to either a commercial recording apparatus (NicoletOne, NATUS, USA) or a custom wireless recording device using snap connectors. Signal to noise values were computed by comparing the maximum signal intensity of the QRS complex to the RMS noise obtained from the baseline signal between subsequent *T* and *P* waves.

ECG Recording. Reference, sensing, and ground electrodes were placed on the torso of alert, healthy volunteers with the reference and ground electrodes placed along the fourth intercostal space to the right and left of the sternum, respectively (V1 and V2 positions in 12-lead precordial placement). The sensing electrode was placed at the fifth intercostal space along the midclavicular line (V4 position in 12 lead placement).[45] ECG validation was conducted with a commercial recording module (NATUS) for a duration of 3 min with the subject in a relaxed sitting position, while long-term stability tests were conducted using a wireless recording module with the same electrode positions for a total duration of 8 h.

EMG Recording. Hydrogel electrodes were placed along the wrist flexors of volunteers to detect an electrical impulse during muscle activation. Muscle flexion was induced by instructing volunteers to grip a small dumbbell (5.4 kg) to induce contraction of the forearm (hand opening/closing). Tests consisted of 8 cycles of contraction/relaxation, each cycle involving 10 s of hand opening, followed by 10 s of hand closing.

EEG Recording. Hydrogel electrodes were placed on the foreheads of healthy volunteers using the 10−20 placement system with sensing and ground electrodes positioned at the Fp1 and Fp2 positions, respectively, and the reference electrode positioned 1 cm below the right mastoid.[46] In a normal experiment, volunteers were placed in a relaxed sitting position and were instructed to sequentially open and close their eyes at intervals of 10 s to induce regular periods of wakeful relaxation. After a total of 5 rounds of eye-opening/closing subjects were instructed to blink 5 times at 1 s intervals to mark the end of the test.

Electrode Stability Tests. The long-term stability of food-based hydrogel electrolytes was interrogated by extended ECG and EEG recordings over the course of a normal workday. ECG experiments were conducted using the wireless recording module described above with participants instructed to wear the device continuously for 8 h during which time data was streamed directly to a nearby Bluetooth-enabled device (Ipad). EEG measurements were also carried out over an 8 h period, albeit not continuously. Electrodes were attached to volunteers, and baseline measurements were performed as described above. The electrodes were left in place, with participants free to perform normal daily activities. EEG measurements were then repeated after 4 and 8 h.

Cost Comparison Analysis. Publicly available list prices were used to compare the cost of starch-based recording electrodes to similar consumables for ECG monitoring, as quoted from the manufacturer. Wherever multiple models were available, the lowest cost was used for comparison. Two types of electrodes were considered in this analysis, the first involving standard, single-use snap-on ECG electrodes compatible with Holter monitoring (a traditional method for continuous monitoring of cardiac function, 3 M Red Dot). The second type involved a newer generation reusable wearable ExG monitoring system, where a single-use adhesive is used (Bittium, OmegaSnap 1-Channel ECG Electrode).

RESULTS AND DISCUSSION

Hydration Structure and Thermal Stability of Food-Based Hydrogels. FTIR spectroscopy (Figure 2c) was used to evaluate the identity and prevalence of functional groups contributing to the ionic conductivity and structural rigidity of starch composite electrolytes. All hydrogels display prominent bands associated with O−H (stretching mode, 3500−3600 cm^{-1}), C−H (stretching mode, 2900−3000 cm^{-1}), and C−O (bending mode, 1600−1650 cm^{-1}) groups along with characteristic C−O−C stretching modes and carbohydrate ring vibrations (800−1200 and 750−900 cm^{-1}, respectively) aligning with previous reports on the spectroscopic and structural characteristics of agricultural starches (Figure S4 provides spectra for all gel compositions).[47] As others have noted, the prevalence of strongly hydrophilic groups (principally O−H and C−O−C residues) within the carbohydrate backbone not only affects rapid hydration/gelation but also imparts high ionic conductivity due to cationic charge hopping along anionic surface sites.[48,49] These features likewise accommodate free water mobility within the starch network benefiting fast ion transport.[50,51] The retention of these structural characteristics following gel formation and the spectroscopic similarity across gels fabricated from different forming polymers reflects the interchangeability of food starches in the fabrication of ionically conductive hydrogel composites.

In addition to its influence on the conductivity and gel formation, the hydrophilicity of processed starches yields hydrogel structures with marked water retention, even at elevated temperatures. This hydration stability is evidenced in Figure 2d wherein representative hydrogel samples were interrogated with thermogravimetric analysis (TGA) under a N_2 atmosphere (for clarity, only optimized compositions are presented here, and TGA traces for all compositions are provided in Figure S5). All samples display modest mass loss (<10%) prior to 180 °C despite aqueous mass fractions near 90% reflecting the structural stability of the hydrated polysaccharide gel. Beyond 180 °C samples display more significant mass loss associated with the bulk removal of

https://doi.org/10.1021/acssuschemeng.4c07823
ACS Sustainable Chem. Eng. 2025, 13, 6051−6063

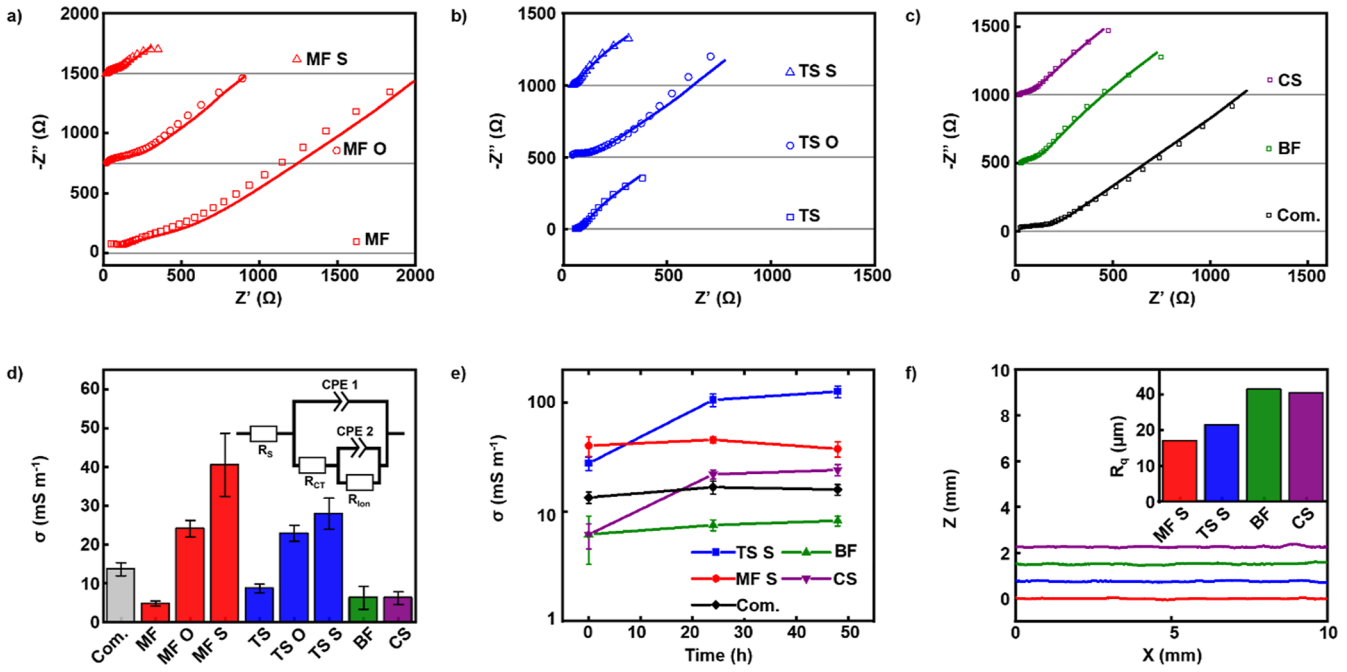

Figure 3. Representative electrochemical impedance spectra obtained from (a) mango flour, (b) tapioca starch, (c) banana flour, corn starch, and commercial electrolytes including real (dotted traces) and simulated (solid traces) spectra. Spectra are shifted vertically by a constant offset for clarity. (d) Ionic conductivities computed for each gel electrolyte using the equivalent circuit model presented as an inset. (e) Variation in ionic conductivity during dry storage. (f) Surface profiles (solid traces) and roughness (inset) of as-prepared hydrogels determined by optical profilometry.

structural water. Significantly, starches fabricated from tapioca and corn feedstocks only display this bulk dehydration above 300 °C. Beyond 300 °C, all samples display slow but progressive mass loss associated with the decomposition of the, now dehydrated, starch backbone.[52] Significantly, starches assembled without glycerol also display elevated hydration stability (albeit with a slightly reduced decomposition temperature, Figure S5c), suggesting that while glycerol does impart some thermal protection, the starch backbone provides significant stabilization.

This hydration stability is further elucidated in room temperature dehydration studies, wherein fresh hydrogel samples were left to dehydrate in a dry-air desiccator with their mass loss monitored by weighing at 24 and 48 h as displayed in Figure 2e. Notably, hydrogel samples fabricated from mango and tapioca starches display mass retention well over 75% even after 48 h dry storage, with banana and corn gels maintaining over 50% within the same period. While the aqueous mass retention of starch-based electrolytes is generally lower than that obtained from commercial PMMA electrolytes, the persistently high ionic conductivities developed by starch composites, even during prolonged storage (vide infra), suggest that the evaporative loss of free water does not negatively impact the functionality of these hydrogel composites. The mass retention of optimized gel compositions is likewise characterized at elevated temperatures (50 °C) as presented in the Supporting Information (Figure S6). While samples stored in open air display lower mass retention than their room temperature counterparts, those stored in covered vessels (close Petri dish) display marked improvements in mas retention, suggesting that proper gel storage may be sufficient to mitigate the deleterious impacts imposed by storage in arid climates.

Mechanical Characterization of Starch Hydrogels. The mechanical characteristics of the hydrogel samples were evaluated by uniaxial elongation at constant velocity to elucidate their elasticity and robustness to physical deformation. Figure 2f presents representative stress−strain curves obtained from as-prepared hydrogels compared against a commercial PMMA gel electrode (stress−strain curves for all samples are provided in Figure S7). Irrespective of forming polymer, starch-based hydrogels display an approximately linear stress/strain relation at low strain, indicative of elastic mechanical deformation.[53] The slope in this linear region was used to quantify the elastic modulus of each material as presented in Figure 2g. While most hydrogels displayed moduli between 2 and 6 kPa, hydrogels formed from corn feedstocks displayed much greater stiffness (>30 kPa). This elevated mechanical stiffness likely stems from the high amylopectin content of waxy corn starch in comparison to the other starches considered here.[54]

Regardless of the modulus, hydrogels undergo rapid failure at elevated strain with very little plastic deformation. Figure 2h presents breaking strains computed from the results displayed in Figure 2f. Interestingly, the breaking strains of hydrogel samples (including those composed of corn starches) are broadly similar to those obtained from commercial PMMA gels, reflecting the robustness of starch-based composites under modest mechanical deformation. This, combined with the similar elastic moduli reported in Figure 2g, substantiates the mechanical compliance of food-based hydrogels as an alternative to conventional electrophysiology recording gels.

Conductivity Analysis of Starch-Based Hydrogels. The ionic conductivities of food-based hydrogels were evaluated by using potentiometric electrochemical impedance spectroscopy. Figure 3a−c displays the EIS spectra (dotted traces) collected from representative hydrogel samples using a

https://doi.org/10.1021/acssuschemeng.4c07823
ACS Sustainable Chem. Eng. 2025, 13, 6051−6063

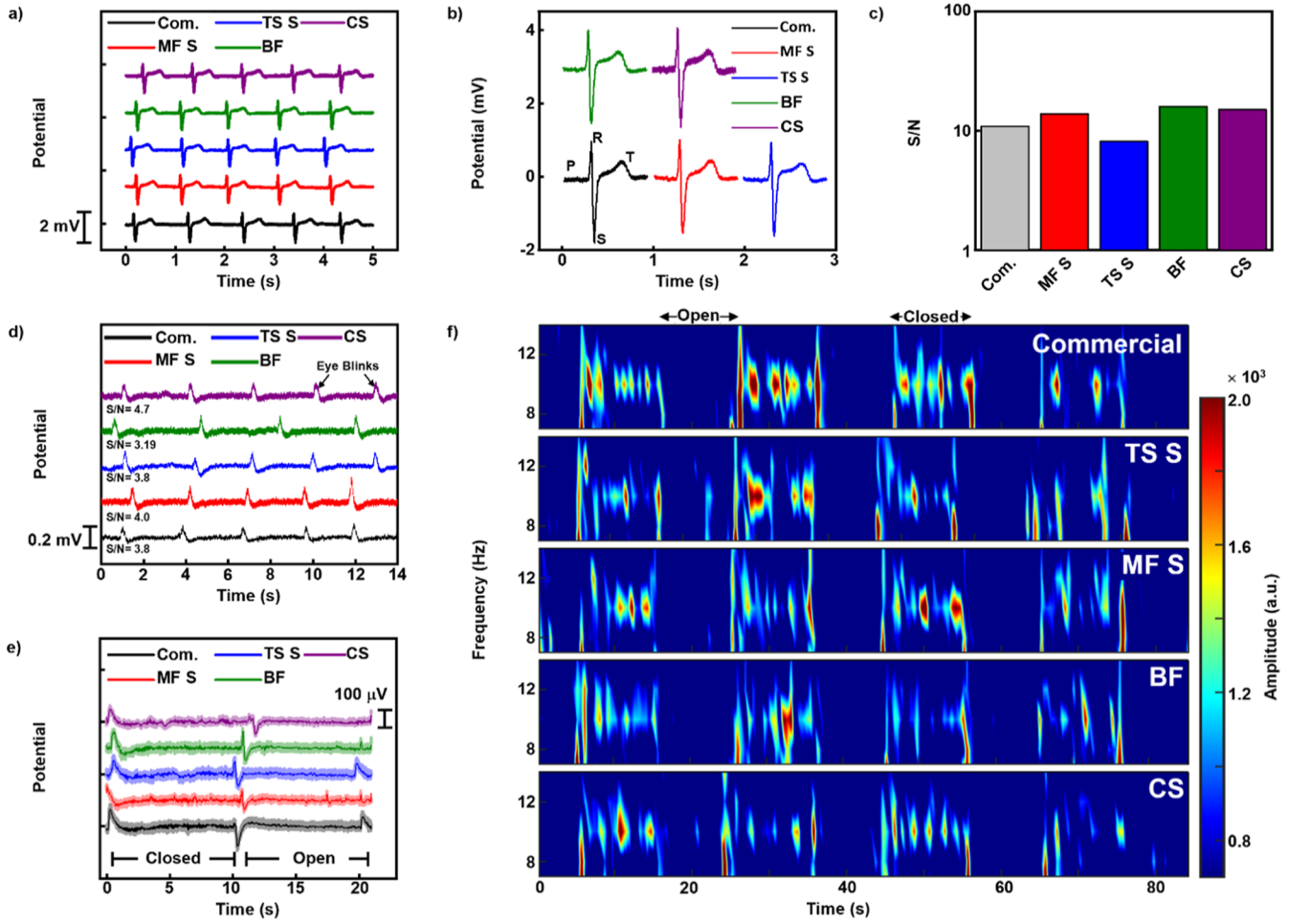

Figure 4. (a) Representative ECG waveforms collected using starch-based gels as the electrolyte. (b) Individual heartbeat waveforms highlighting the differentiation of polarization/depolarization events characteristic of healthy cardiac rhythm. (c) Signal-to-noise characteristics of ECG data collected using starch-based electrolytes. (d) EEG waveforms collected during participant blinking using starch-based composites as the electrolyte. Signal-to-noise characteristics are presented below each trace. (e) EEG data collected from a participant while sequentially opening and closing their eyes. Shaded traces present the raw data with solid traces depicting data after Fourier filtering to remove interference from frequencies greater than 40 Hz. (f) Spectrograms computed from a time series of 5 periods of eye opening and closing illustrating the appearance of intensity near 10 Hz during periods of wakeful relaxation associated with the presence of alpha rhythms.

pair of Ag/AgCl stimulating electrodes. Raw EIS data was analyzed with an equivalent circuit model (solid traces) to extract the bulk ionic conductivity of hydrogel composites. Data presented in Figures 3a–c are stacked vertically for visualization by using a constant offset.

Irrespective of forming polymer, hydrogel composites exhibit similar features in their Nyquist impedance including a high-frequency semicircle associated with the AgCl/hydrogel interface and a low-frequency tail attributed to bulk ion transport across the hydrogel sample. These features are quantified using the modified Randle's circuit provided as an inset of Figure 3d. While the traditional Randle's circuit, consisting of a single capacitive interface and constant phase Warburg diffusion element, is effective at modeling ion transport through a semi-infinite ionic media, it cannot accommodate the high conductivities and short diffusion distances associated with these thin (ca. 3 mm) hydrogel electrolytes. To address this deficiency, a modified constant phase element was used in place of a Warburg element to more accurately treat confined ion diffusion as discussed elsewhere.[43]

Ionic conductivities extracted from equivalent circuit fitting are presented in Figure 3d for each starch hydrogel. Notably, the composition of hydrogel samples plays a significant role in mediating ion transport through the bulk electrolyte. Hydrogels prepared without a plasticizer and with low salt contents display modest ionic conductivities associated with sluggish charge transport across the bulk gel. Upon the addition of an oil plasticizer (MF O and TS O), the ionic conductivity increases likely due to greater chain mobility accelerating charge hopping along the carbohydrate backbone.[55] Likewise, increasing NaCl loading (MF S and TS S) raises the ionic conductivity of the gel due to a greater prevalence of mobile ions accommodating charge transport, as displayed in Figure 3d. Significantly, all samples considered here display ionic conductivities between 5 and 50 mS m^{-1}, meeting or exceeding the conductivity of comparable polyelectrolyte hydrogels.[56] Due to the high ionic conductivities obtained from NaCl-rich gels, these electrolyte compositions were chosen for subsequent ExG studies. Similarly, starch-based hydrogels display excellent linearity and stability in response to applied excitation pulses, as presented in the Supporting Information (Figure S8).

The long-term stabilities of gel samples were also characterized by EIS to quantify any putative effect of

https://doi.org/10.1021/acssuschemeng.4c07823
ACS Sustainable Chem. Eng. 2025, 13, 6051−6063

dehydration on ion transport. Samples were stored, uncovered, at room temperature with EIS performed at 24 h intervals. Figure 3e presents the conductivities of these samples, displaying only modest changes in ionic transport over the course of several days of dry storage. Interestingly, all hydrogel samples exhibit increases in ionic conductivity during storage, possibly due to polymer relaxation, or increases in NaCl concentration during dehydration, analogous to the changes presented in Figure 3d at elevated NaCl loadings. Interestingly, the magnitude of this effect varies across different starches and is most likely due to mechanical changes to gel composites with aging. While gels composed of mango and banana flour display little change in their mechanical behavior with time, those composed of tapioca and corn starches soften significantly with aging (Figure S9). This softening increases chain mobility, thereby improving the ionic conductivity. In addition to ionic conductivity, the contact impedance of hydrogel electrodes during dry storage shows only a modest increase over the course of 48 h, reflecting the robust electrical and interfacial characteristics of starch-based composites (Figure S10).

In addition to the maintenance of high bulk ionic conductivity during dry storage, starch-based electrolytes retain stable and low interfacial impedance during extended storage (Figure S11) and display no visible deleterious effect on Ag/AgCl electrodes with prolonged contact (Figure S12), reflecting the interfacial stability of this electrolyte system. Similarly, the surface roughness of the hydrogel samples was characterized with optical profilometry, the results of which are provided in Figure 3f. All samples display low RMS roughness between 10 and 40 μm. This low interfacial roughness, coupled with the low moduli of food starch gels, supports the formation of favorable interfacial contact between the gel and Ag/AgCl recording electrodes as well as between the gel and the skin surface.

ExG Recording with Hydrogel Electrolytes. The efficacy of optimized starch-based hydrogels as signal transducers for biopotential recording was characterized by a series of electrophysiology measurements on healthy volunteers using a commercial recording system (Nicolet1, Natus). A low-cost (ca. 0.025 USD per electrode) fabrication approach was used to connect starch-based hydrogels to reusable snap electrodes, facilitating communication between the hydrogel surface and the recording apparatus (Figure S2). Figure 4a presents 3-electrode ECG waveforms collected using commercial PMMA-based electrolyte gels as well as data collected using food-based hydrogel electrolytes. All samples display clearly differentiated P and T waves associated with arterial depolarization and ventricular repolarization, respectively, as well as a prominent QRS complex resulting from ventricular depolarization.[57] These features are highlighted in Figure 4b and are associated with a normal cardiac rhythm. As evidenced by the results displayed in Figure 4a,b, ECG waveforms collected using food-based hydrogels agree strongly with equivalent waveforms obtained using the commercial standard electrode gel (black trace). In addition to the deconvolution of characteristic depolarization/repolarization waves, starch-based hydrogels display favorable signal-to-noise characteristics, with all hydrogels displaying S/N ratios near 10 as calculated by comparing the maximum intensity of the QRS complex to the baseline RMS noise of each gel (Figure 4c). Notably, these S/N ratios are comparable to those obtained from other advanced electrolyte formulations including formulations based on (polyethylene glycol) diacrylate, polypyrrole, or poly(3,4-ethylenedioxythiophene)/polystyrenesulfonate.[58−60]

The signal quality obtained from hydrogel composites was further evaluated with three-electrode EEG as displayed in Figure 4d−f. Participants were first prompted to blink sequentially at one s intervals to evaluate electrode responses to reflexive eye movement during eyelid motion (Bell's phenomenon). Results of this measurement protocol are displayed in Figure 4d wherein polarization waves are obtained in direct alignment with patient blinking indicating the capacity of hydrogel electrodes to record large changes to local biopotentials. The S/N ratios associated with blinking (displayed below each trace in Figure 4d) were used to evaluate the quality of the hydrogel contacts. Similar to results obtained from ECG waveforms, the S/N characteristics obtained from food-based hydrogels agree well with results obtained from a commercial electrode.

Following eye-blinking, participants were instructed to open and close their eyes at 10 s intervals to stimulate the characteristic alpha rhythm associated with wakeful relaxation. Figure 4e presents the raw (light color) and Fourier-filtered (bold color, cutoff frequency = 40 Hz) EEG data obtained from sequential eye opening and closing. All gel electrodes display additional EEG features when participants' eyes are closed due to the superposition of additional sinus rhythms (principally the alpha rhythm) to the baseline EEG characteristic. To reinforce this assignment, Fast Fourier analysis was used to spectrally decompose EEG data in the frequency domain to assign a waveform amplitude to each frequency component contributing to the signals displayed in Figure 4e. The results of this analysis are presented as amplitude spectrograms in Figure 4f for a total of 5 periods of eye opening and closing. In agreement with the results described in Figure 4e, spectrograms display increased intensity at high frequency when the eyes are closed relative to the period when the eyes are open. Moreover, the characteristic frequency of these additional component waveforms occurs between 8 and 12 Hz, aligning well with the common frequency band associated with alpha rhythm.[61]

Overall, the results presented in Figure 4 demonstrate that hydrogel electrolytes are capable of recording high-quality ExG data in myriad contexts. Interestingly, signal quality appears independent of the forming polymer or the plasticizer used in electrode assembly. This insensitivity is attributed to the high NaCl loading and, therefore, the high ionic conductivity of starch-based composite electrodes. While different starches present different ratios of amylose to amylopectin (impacting hydration, mechanical stability, and plasticizer solubility), these differences do not hinder ion conduction and, by extension, signal transduction across the gel electrolyte. This is most apparent for corn-based hydrogels whose mechanical properties differ markedly from other composites (Figure 2g), while still delivering comparable EXG performance due to the maintenance of favorable interfacial contact with human skin. These results demonstrate the versatility of starch-based composites as EXG electrolytes, as they can accommodate many different combinations of starch and plasticizer without sacrificing signal quality.

Long-Term Wireless Recording of ExG Signals Using Starch-Based Hydrogels. To demonstrate the capability for widespread deployability of the food-based hydrogels described above, hydrogel electrodes were coupled to a custom-built wireless recording platform capable of high-

https://doi.org/10.1021/acssuschemeng.4c07823
ACS Sustainable Chem. Eng. 2025, 13, 6051−6063

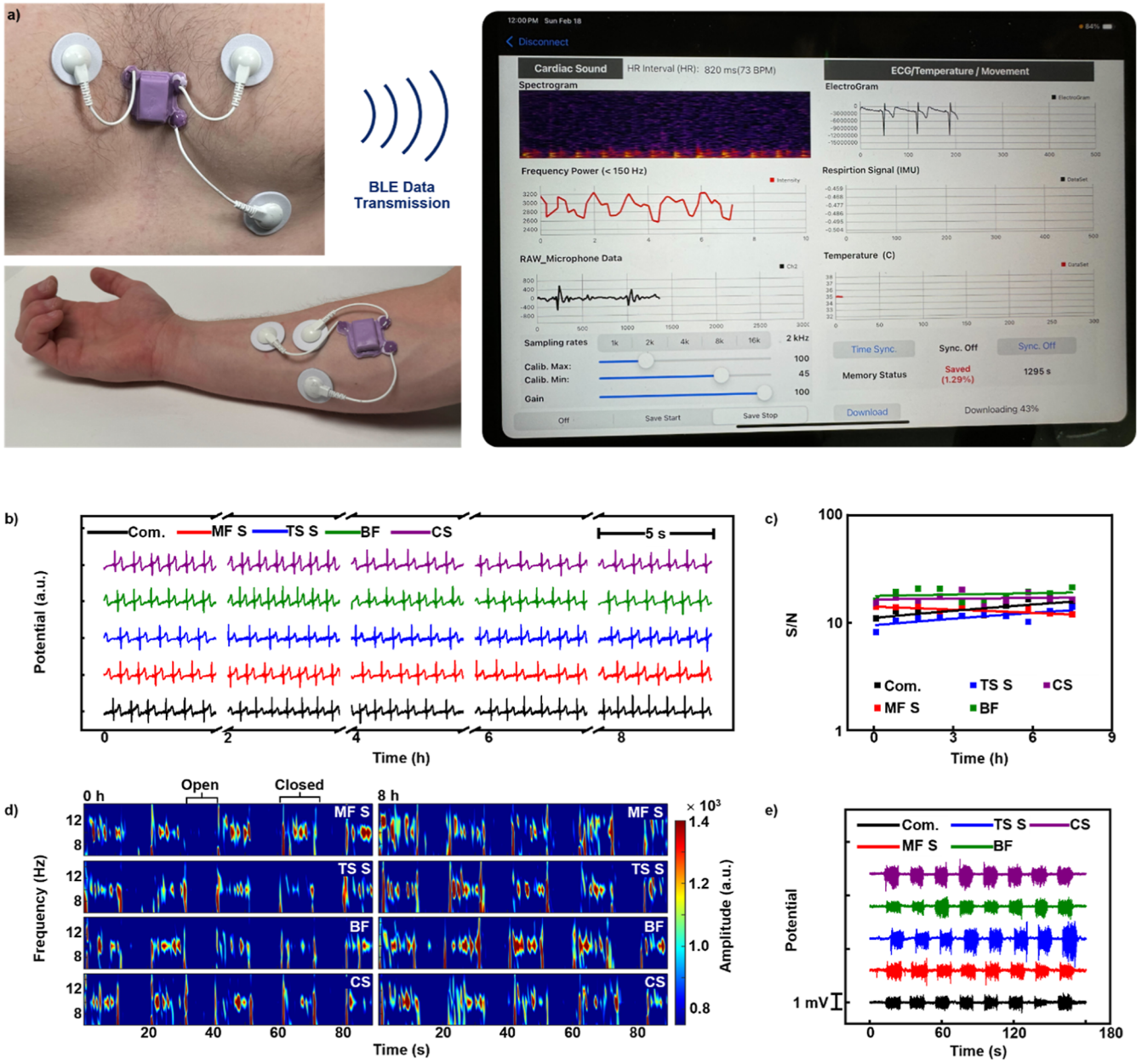

Figure 5. (a) Photographs depicting the application of the wireless recording device on different areas of the body and the transmission of live data from the device to a mobile recording application. (b) Long-term continuous ECG recording using the wireless recording platform and starch-based gel electrolytes. Data displays 5 s snapshots separated by 2 h intervals. (c) Signal-to-noise computed from the waveform data presented in (b). (d) Spectrograms obtained from EEG recording over an 8 h period demonstrating the isolation of alpha rhythm characteristics near 10 Hz. (e) Electromyography collected from the forearm during repeated hand contraction.

quality data acquisition/streaming via the Bluetooth low-energy (BLE) protocol. The system, pictured in Figure 5a, accommodates ECG and EMG recording with simultaneous data visualization through a communication/processing application running simultaneously on a Bluetooth-enabled mobile device (Ipad). The lightweight construction and small footprint of the wireless recording module permit continuous ExG recording over long stretches of time without encumbering the user. To this end, the extended stability of ECG recording with starch hydrogel electrodes were interrogated by continuous ECG logging over 8 h.

Figure 5b displays representative waveforms obtained during long-term ECG recording using the wireless platform normalized by the maximum intensity obtained from the QRS complex (Table S2). Regardless of gel composition, the results obtained from the wireless platform agree well with analogous measurements conducted using a commercial recording apparatus (Figure 4a,b). Likewise, signal integrity remains stable, with negligible potentiometric drift over the entire duration of recording. Figure 5c presents S/N characteristics of hydrogel samples throughout the recording period, displaying negligible decay in signal quality due to gel dehydration. Indeed, the S/N characteristics of starch-based hydrogels are nearly identical to those of commercial electrode gel, suggesting that limits on signal quality are principally a result of the recording system rather than the gel electrolytes. Importantly, due to the adhesive contact formed between the electrode housing and the skin, hydrogels are maintained in an

https://doi.org/10.1021/acssuschemeng.4c07823
ACS Sustainable Chem. Eng. 2025, 13, 6051−6063

approximately sealed environment, reducing deleterious moisture loss from the composite.

In tandem with long-term ECG recording, the biocompatibility of hydrogel electrolytes is evaluated by inspection of participants' skin at regular time intervals during extended wear. Figure S13 displays representative images collected from the forearm of a healthy participant before the application of hydrogel electrolytes, and at 6 and 12 h of continuous wear. No obvious dermal irritation is visible during extended skin contact, likewise participants report no discomfort associated with hydrogel electrolytes during the testing period. These results support the biocompatibility of the starch-based electrolyte composites considered in this investigation. Additionally, accelerated aging tests in phosphate-buffered saline (Figure S14) demonstrate the environmental compatibility of starch-based hydrogels, each of which dissolved harmlessly over a period of several days.

To further evaluate signal evolution over long recording times, EEG data were collected over a period of 8 h, leaving the hydrogel electrodes in place between measurements. Figure 5d displays the results of this characterization with a principal focus on the deconvolution of subtle alpha rhythms by Fourier analysis. As evidenced by prominent increases in signal amplitude around 10 Hz in all samples during wakeful relaxation, irrespective of time, gel electrodes retain sufficient conductivity and interfacial stability to characterize subtle EEG signals even after 8 h of continuous wear (Figure S15 provides analogous results obtained from a commercial gel). Finally, to demonstrate the versatility of the wireless recording platform, EMG waveforms were collected along the forearm flexors of healthy participants. Figure 5e presents raw EMG waveforms for a series of repeated hand contractions with computed activation envelopes provided in Figure S16. Taken together, this data supports the versatility and stability of both the wearable platform and the starch-based hydrogel electrolytes for the continuous recording of biopotential data with low material cost and potential widespread deployability.

Impact of External Factors on ECG Signal Quality. In addition to long-term storage, the susceptibility of hydrogel electrodes to motion artifacts is also an important practical consideration. Figure S17 presents ECG wave forms obtained from hydrogel electrodes both at rest and during periodic rotator cuff motion to simulate real-world motion artifacts. Irrespective of gel composition, all electrodes display only a modest signal change under external motion, with the most prominent difference being a slight increase in RMS noise under periods of rotation. Despite this increase, signals remain clear and well resolved, suggesting that hydrogel electrodes are adequately stable against deleterious subject motion. Further, ECG waveforms collected during compressive, tensile, and shearing deformation (10% strain, Figure S18) demonstrate no significant changes in signal quality relative to unstrained electrolytes (Figure S19).

Beyond motion artifacts, the stability of gel electrodes during subject sweating is likewise quantified with ECG measurements on healthy subjects both under ambient conditions and in a dry sauna to induce a sweat response. Figure S20 presents representative ECG waveforms obtained during these measurements, showing a negligible change between signals collected under normal conditions and those collected during sweating. These results support the use of hydrogel electrodes on subjects during exercise and/or in warm climates where significant sweating may be unavoidable. Finally, the reusability of hydrogel electrodes is considered by removing and reapplying gel electrolytes to healthy human participants. Figure S21 presents the results of these measurements, demonstrating no significant change in signal RMS on reuse. Importantly, these measurements only consider the reusability of the gel itself (medical adhesive was replaced with each reapplication to maintain intimate contact between the electrode and the skin).

Adhesive-Free ECG Recording with Hydrogel Electrolytes Using a Low-Cost Harness. Despite the already low cost of the recording electrodes detailed above, the use of double-sided medical adhesive could prove to be prohibitive in some locations. Similarly, the composite gel electrolytes considered here are not sufficiently adhesive to independently anchor recording apparatus to the body (Figure S22). To circumvent this limitation, hydrogel electrolytes are integrated into a low-cost (total materials cost ca. 1.27 USD, excluding snap electrodes), reusable, adhesive-free harness, as depicted in Figure S23. The harness, composed primarily of EVA foam and aluminum armature wire, can be fully assembled by hand and can be shaped to conform to individual users to provide high-quality ECG recording. This combination of a reusable wireless recording module and low-cost, reusable EXG harness reduces the price per electrode from 0.025 USD to only 0.004 USD, without necessitating specialty materials or processing.

Cost Comparison Analysis. Even with a significant profit margin (50%), starch-based hydrogels would be highly cost-effective compared to existing solutions. Table 1 demonstrates

Table 1. Price Comparison between Starch-Based and Commercially Available ECG Electrodes

electrode type	starch-based	starch-based (no adhesive)	3 M red dot	Bittium OmegaSnap
monitoring equipment	ANNE chest	ANNE chest + harness	Holter monitor	Bittium
price per unit (USD)	0.0375[a]	0.006[a]	0.41[b]	14.15
cost savings (%)			89.0	99.7

[a]Assumes a 50% profit margin on top of the cost to account for packaging, marketing, sales, and distribution. [b]Typically requires 3 per monitoring session to operate with Holter monitoring solutions.

that by reverting to starch-based consumables, the cost per monitoring solution would be 89% lower when compared to traditional snap electrodes and 99.7% lower when compared to a wearable medical patch. Further reductions in cost can be realized by switching to an adhesive-free electrode assembly using a reusable recording harness. Likewise, more than 300 million ECGs are performed worldwide each year; thus, the potential global cost savings for starch-based electrodes would approach 328 million dollars per annum. This impact could be especially profound in resource-limited settings, where there is tremendous unmet demand for cardiac services.[62]

Sustainability, Medical Waste, and Local Manufacturing Opportunities. Hospitals in the United States account for 4 million tons of general waste each year.[63] Disposable material, specifically plastic packaging and single-use devices, drives the majority of medical waste, while it is unknown how much ECG-related consumables contribute to this total, starch-based hydrogels offer a more sustainable approach for ECG monitoring, as they likely will require less specialized handling and are naturally biodegradable. The COVID-19

https://doi.org/10.1021/acssuschemeng.4c07823
ACS Sustainable Chem. Eng. 2025, 13, 6051−6063

pandemic illustrated the profound fragility of global supply chains for low- and middle-income countries, where the availability of essential medical technology was severely strained.[64] By leveraging widely available local materials, starch-based hydrogels represent economic opportunities by creating opportunities for local manufacturing in the future.

CONCLUSIONS

Herein, we disclose composite hydrogel electrolytes fabricated from low-cost, readily available agricultural feedstocks with high ionic conductivity, mechanical stability, and dehydration resistance. We demonstrate their proficiency as high-quality electrolytes for ExG recording with performances that rival those of commercially available PMMA-based recording gels. Likewise, we demonstrate their long-term efficacies, realizing low-noise continuous ECG data acquisition for up to 8 h. Finally, we demonstrate the versatility and deployability of these electrodes by paring them with a small, lightweight, wireless recording module affecting both ECG and EMG recording in remote settings. More broadly, this work illustrates the importance of local agricultural byproducts as key chemical feedstocks for biomedical applications and offers new opportunities toward the widespread proliferation of clinical grade biomedical technologies in resource-limited settings by reducing the cost compared to existing solutions and supporting sustainability.

ASSOCIATED CONTENT

Supporting Information

The Supporting Information is available free of charge at https://pubs.acs.org/doi/10.1021/acssuschemeng.4c07823.

Viscosity measurements of hydrogel precursor solutions; schematic illustration of low-cost hydrogel electrodes; detailed electrode cost analysis; ECG normalization coefficients; additional thermal, mechanical, and electronic characterization; signal linearity measurements; characterization of electrode/electrolyte interfaces; contact impedance measurements; dermal compatibility; biodegradability; analysis of motion artifacts; analysis of deformation artifacts; analysis of electrode reusability; analysis of stability on body during sweating; skin adhesion measurements; long-term EEG recording from a commercial electrolyte; computed EMG envelopes collected from the wireless recording platform; and construction and performance of an adhesive-free ECG harness (PDF)

AUTHOR INFORMATION

Corresponding Author

John A. Rogers − *Querrey Simpson Institute for Bioelectronics, Northwestern University, Evanston, Illinois 60208, United States; Department of Materials Science and Engineering and Department of Biomedical Engineering, Northwestern University, Evanston, Illinois 60208, United States; Department of Neurological Surgery, Feinberg School of Medicine, Northwestern University, Chicago, Illinois 60611, United States;* orcid.org/0000-0002-2980-3961; Email: jrogers@northwestern.edu

Authors

Lilian C. Alarcón-Segovia − *Querrey Simpson Institute for Bioelectronics, Northwestern University, Evanston, Illinois 60208, United States; Núcleo de Innovación Médica, Facultad de Medicina, Universidad María Auxiliadora, Asunción 2040, Paraguay; Instituto de Matemática Aplicada del Litoral, Universidad Nacional del Litoral and Consejo Nacional de Investigaciones, Científicas y Técnicas, Santa Fe 3000, Argentina*

Kenneth E. Madsen − *Querrey Simpson Institute for Bioelectronics, Northwestern University, Evanston, Illinois 60208, United States; Department of Chemistry, University of Illinois at Urbana−Champaign, Urbana, Illinois 61801, United States;* orcid.org/0000-0002-1336-567X

Claire Liu − *Querrey Simpson Institute for Bioelectronics, Northwestern University, Evanston, Illinois 60208, United States; Chan Zuckerberg Biohub Chicago, Chicago, Illinois 60642, United States;* orcid.org/0000-0003-4308-389X

Sun Hong Kim − *Querrey Simpson Institute for Bioelectronics, Northwestern University, Evanston, Illinois 60208, United States*

Tae Wan Park − *Querrey Simpson Institute for Bioelectronics, Northwestern University, Evanston, Illinois 60208, United States*

Yayun Du − *Querrey Simpson Institute for Bioelectronics, Northwestern University, Evanston, Illinois 60208, United States*

Joanna L. Ciatti − *Querrey Simpson Institute for Bioelectronics, Northwestern University, Evanston, Illinois 60208, United States; Department of Materials Science and Engineering, Northwestern University, Evanston, Illinois 60208, United States;* orcid.org/0000-0001-5393-522X

Kathrin H. Salame − *Querrey Simpson Institute for Bioelectronics, Northwestern University, Evanston, Illinois 60208, United States*

Jae-Young Yoo − *Department of Semiconductor Convergence Engineering, Sungkyunkwan University, Suwon 16419, Republic of Korea*

Complete contact information is available at: https://pubs.acs.org/10.1021/acssuschemeng.4c07823

Author Contributions

♦L.C.A.-S. and K.E.M. contributed equally to this work.

Notes

The authors declare the following competing financial interest(s): J.A.R. is a co-founder and advisor to Sibel Health and holds patents associated with this company.

ACKNOWLEDGMENTS

This work was supported by the Querrey-Simpson Institute for Bioelectronics at Northwestern University. K.E.M. acknowledges the support from an NIH sleep and circadian training grant (T32HL007909). LCAS acknowledges the support from BECAL, Paraguay, Universidad Maria Auxiliadora, Paraguay. Instituto de Matemática Aplicada del Litoral, Universidad Nacional del Litoral and Consejo Nacional de Investigaciones, Científicas y Técnicas, Argentina. J.L.C. graciously acknowledges the support from the National Science Foundation Graduate Research Fellowship under Grant no. DGE-2234667. This work made use of the EPIC facility of Northwestern University's NUANCE Center, which has received support from the SHyNE Resource (NSF ECCS-2025633), the IIN, and Northwestern's MRSEC program (NSF DMR-2308691). Figures 1a,b,e and 2a and the TOC image were partially

created in BioRender. Madsen, K. (2025) https://BioRender.com/eec2jms (agreement number: CH285BGJUV).

REFERENCES

(1) Ha, S.; Kim, C.; Wang, H.; Chi, Y. M.; Mercier, P. P.; Cauwenberghs, G. Chapter 6 - Low-power integrated circuits for wearable electrophysiology. In *Wearable Sensors*, 2nd ed.; Sazonov, E., Ed.; Academic Press: Oxford, 2021; pp 163−199.

(2) Imani, S.; Bandodkar, A. J.; Mohan, A. M. V.; Kumar, R.; Yu, S.; Wang, J.; Mercier, P. P. A wearable chemical−electrophysiological hybrid biosensing system for real-time health and fitness monitoring. *Nat. Commun.* **2016**, *7* (1), 11650.

(3) Tian, L.; Zimmerman, B.; Akhtar, A.; Yu, K. J.; Moore, M.; Wu, J.; Larsen, R. J.; Lee, J. W.; Li, J.; Liu, Y.; Metzger, B.; Qu, S.; Guo, X.; Mathewson, K. E.; Fan, J. A.; Cornman, J.; Fatina, M.; Xie, Z.; Ma, Y.; Zhang, J.; Zhang, Y.; Dolcos, F.; Fabiani, M.; Gratton, G.; Bretl, T.; Hargrove, L. J.; Braun, P. V.; Huang, Y.; Rogers, J. A. Large-area MRI-compatible epidermal electronic interfaces for prosthetic control and cognitive monitoring. *Nat. Biomed. Eng.* **2019**, *3* (3), 194−205.

(4) King, C. E.; Sarrafzadeh, M. A Survey of Smartwatches in Remote Health Monitoring. *J. Healthc. Inform. Res.* **2018**, *2* (1), 1−24.

(5) Chandel, R. S.; Sharma, S.; Kaur, S.; Singh, S.; Kumar, R. Smart watches: A review of evolution in bio-medical sector. *Mater. Today: Proc.* **2022**, *50*, 1053−1066.

(6) Asgari Mehrabadi, M.; Azimi, I.; Sarhaddi, F.; Axelin, A.; Niela-Vilén, H.; Myllyntausta, S.; Stenholm, S.; Dutt, N.; Liljeberg, P.; Rahmani, A. M. Sleep tracking of a commercially available smart ring and smartwatch against medical-grade actigraphy in everyday settings: instrument validation study. *JMIR mHealth and uHealth* **2020**, *8* (10), No. e20465.

(7) Nguyen, S.; Duong, C.; Amirtharajah, R. A Smart Health Tracking Ring Powered by Wireless Power Transfer. *2021 IEEE Wireless Power Transfer Conference (WPTC)*; IEEE, 2021, pp 1−4. 1−4 June 2021.

(8) Zhu, M.; Sun, Z.; Zhang, Z.; Shi, Q.; He, T.; Liu, H.; Chen, T.; Lee, C. Haptic-feedback smart glove as a creative human-machine interface (HMI) for virtual/augmented reality applications. *Sci. Adv.* **2020**, *6* (19), No. eaaz8693.

(9) Chouhan, T.; Panse, A.; Voona, A. K.; Sameer, S. M. Smart glove with gesture recognition ability for the hearing and speech impaired. *2014 IEEE Global Humanitarian Technology Conference—South Asia Satellite (GHTC-SAS)*; IEEE, 2014, pp 105−110. 26−27 Sept. 2014.

(10) Kim, D.; Choi, Y. Applications of Smart Glasses in Applied Sciences: A Systematic Review. *Appl. Sci.* **2021**, *11* (11), 4956.

(11) Maruyama, K.; Watanabe, E.; Kin, T.; Saito, K.; Kumakiri, A.; Noguchi, A.; Nagane, M.; Shiokawa, Y. Smart Glasses for Neuro-surgical Navigation by Augmented Reality. *Operat. Neurosurg.* **2018**, *15* (5), 551−556.

(12) Caeiro-Rodríguez, M.; Otero-González, I.; Mikic-Fonte, F. A.; Llamas-Nistal, M. A Systematic Review of Commercial Smart Gloves: Current Status and Applications. *Sensors* **2021**, *21* (8), 2667.

(13) Kim, D.-H.; Lu, N.; Ma, R.; Kim, Y.-S.; Kim, R.-H.; Wang, S.; Wu, J.; Won, S. M.; Tao, H.; Islam, A.; Yu, K. J.; Kim, T.-i.; Chowdhury, R.; Ying, M.; Xu, L.; Li, M.; Chung, H.-J.; Keum, H.; McCormick, M.; Liu, P.; Zhang, Y.-W.; Omenetto, F. G.; Huang, Y.; Coleman, T.; Rogers, J. A. Epidermal Electronics. *Science* **2011**, *333* (6044), 838−843.

(14) Han, N.; Yao, X.; Wang, Y.; Huang, W.; Niu, M.; Zhu, P.; Mao, Y. Recent Progress of Biomaterials-Based Epidermal Electronics for Healthcare Monitoring and Human−Machine Interaction. *Biosensors* **2023**, *13* (3), 393.

(15) Jeong, J.-W.; Kim, M. K.; Cheng, H.; Yeo, W.-H.; Huang, X.; Liu, Y.; Zhang, Y.; Huang, Y.; Rogers, J. A. Capacitive Epidermal Electronics for Electrically Safe, Long-Term Electrophysiological Measurements. *Adv. Healthcare Mater.* **2014**, *3* (5), 642−648.

(16) Iqbal, S. M. A.; Mahgoub, I.; Du, E.; Leavitt, M. A.; Asghar, W. Advances in healthcare wearable devices. *npj Flexible Electron.* **2021**, *5* (1), 9.

(17) Kamga, P.; Mostafa, R.; Zafar, S. The Use of Wearable ECG Devices in the Clinical Setting: a Review. *Curr. Emerg. Hosp. Med. Rep.* **2022**, *10* (3), 67−72.

(18) Walker, B. A.; Khandoker, A. H.; Black, J. In Low cost ECG monitor for developing countries, *2009 International Conference on Intelligent Sensors, Sensor Networks and Information Processing (ISSNIP)*; IEEE, 7−10 Dec. 2009; 2009; pp 195−199.

(19) Research and Markets *Wearable Patch Global Strategic Business Report*; Online, 2024.

(20) Bouzid, Z.; Al-Zaiti, S. S.; Bond, R.; Sejdić, E. Remote and wearable ECG devices with diagnostic abilities in adults: A state-of-the-science scoping review. *Heart Rhythm* **2022**, *19* (7), 1192−1201.

(21) Al-Ayyad, M.; Owida, H. A.; De Fazio, R.; Al-Naami, B.; Visconti, P. Electromyography Monitoring Systems in Rehabilitation: A Review of Clinical Applications, Wearable Devices and Signal Acquisition Methodologies. *Electronics* **2023**, *12* (7), 1520.

(22) He, C.; Chen, Y. Y.; Phang, C. R.; Stevenson, C.; Chen, I. P.; Jung, T. P.; Ko, L. W. Diversity and Suitability of the State-of-the-Art Wearable and Wireless EEG Systems Review. *IEEE J. Biomed. Health Inform.* **2023**, *27* (8), 3830−3843.

(23) Romero, F. J.; Castillo, E.; Rivadeneyra, A.; Toral-Lopez, A.; Becherer, M.; Ruiz, F. G.; Rodriguez, N.; Morales, D. P. Inexpensive and flexible nanographene-based electrodes for ubiquitous electro-cardiogram monitoring. *npj Flexible Electron.* **2019**, *3* (1), 12.

(24) Greene, J.; Skolnik, C. L.; Merritt, M. W. How medicine becomes trash: disposability in health care. *Lancet* **2022**, *400* (10360), 1298−1299.

(25) Liu, H.; Li, M.; Ouyang, C.; Lu, T. J.; Li, F.; Xu, F. Biofriendly, Stretchable, and Reusable Hydrogel Electronics as Wearable Force Sensors. *Small* **2018**, *14* (36), 1801711.

(26) Wan, R.; Yu, J.; Quan, Z.; Ma, H.; Li, J.; Tian, F.; Wang, W.; Sun, Y.; Liu, J.; Gao, D.; Xu, J.; Lu, B. A reusable, healable, and biocompatible PEDOT:PSS hydrogel-based electrical bioadhesive interface for high-resolution electromyography monitoring and time−frequency analysis. *Chem. Eng. J.* **2024**, *490*, 151454.

(27) Wang, Y.; Huang, H.; Wu, J.; Han, L.; Yang, Z.; Jiang, Z.; Wang, R.; Huang, Z.; Xu, M. Ultrafast Self-Healing, Reusable, and Conductive Polysaccharide-Based Hydrogels for Sensitive Ionic Sensors. *ACS Sustainable Chem. Eng.* **2020**, *8* (50), 18506−18518.

(28) Xiang, H.; Li, Z.; Liu, H.; Chen, T.; Zhou, H.; Huang, W. Green flexible electronics based on starch. *npj Flexible Electron.* **2022**, *6* (1), 15.

(29) Apriyanto, A.; Compart, J.; Fettke, J. A review of starch, a unique biopolymer − Structure, metabolism and in planta modifications. *Plant Sci.* **2022**, *318*, 111223.

(30) Qamruzzaman, M.; Ahmed, F.; Mondal, M. I. H. An Overview on Starch-Based Sustainable Hydrogels: Potential Applications and Aspects. *J. Polym. Environ.* **2022**, *30* (1), 19−50.

(31) Cui, C.; Jia, Y.; Sun, Q.; Yu, M.; Ji, N.; Dai, L.; Wang, Y.; Qin, Y.; Xiong, L.; Sun, Q. Recent advances in the preparation, characterization, and food application of starch-based hydrogels. *Carbohydr. Polym.* **2022**, *291*, 119624.

(32) Elvira, C.; Mano, J. F.; San Román, J.; Reis, R. L. Starch-based biodegradable hydrogels with potential biomedical applications as drug delivery systems. *Biomaterials* **2002**, *23* (9), 1955−1966.

(33) Koshenaj, K.; Ferrari, G. A Comprehensive Review on Starch-Based Hydrogels: From Tradition to Innovation, Opportunities, and Drawbacks. *Polymers* **2024**, *16* (14), 1991.

(34) Messner, R.; Johnson, H.; Richards, C. From surplus-to-waste: A study of systemic overproduction, surplus and food waste in horticultural supply chains. *J. Clean. Prod.* **2021**, *278*, 123952.

(35) Rodrigues, J. P. B.; Liberal, Â.; Petropoulos, S. A.; Ferreira, I. C. F. R.; Oliveira, M. B. P. P.; Fernandes, Â.; Barros, L. Agri-Food Surplus, Waste and Loss as Sustainable Biobased Ingredients: A Review. *Molecules* **2022**, *27* (16), 5200.

(36) Phiri, R.; Mavinkere Rangappa, S.; Siengchin, S. Agro-waste for renewable and sustainable green production: A review. *J. Clean. Prod.* **2024**, *434*, 139989.

https://doi.org/10.1021/acssuschemeng.4c07823
ACS Sustainable Chem. Eng. 2025, 13, 6051−6063

(37) Xu, W.; Yang, H.; Zeng, W.; Houghton, T.; Wang, X.; Murthy, R.; Kim, H.; Lin, Y.; Mignolet, M.; Duan, H.; Yu, H.; Slepian, M.; Jiang, H. Food-Based Edible and Nutritive Electronics. *Adv. Mater. Technol.* **2017**, *2* (11), 1700181.
(38) Sharova, A. S.; Melloni, F.; Lanzani, G.; Bettinger, C. J.; Caironi, M. Edible Electronics: The Vision and the Challenge. *Adv. Mater. Technol.* **2021**, *6* (2), 2000757.
(39) Vilpoux, O. F.; Santos Silveira Junior, J. F. Chapter 3 - Global production and use of starch. In *Starchy Crops Morphology, Extraction, Properties and Applications*; Pascoli Cereda, M., François Vilpoux, O., Eds.; Academic Press, 2023; pp 43−66.
(40) Tang, M.; Wang, Y.; Niu, X.; Liu, D. Morphological characteristics of starch sol-gel and its influences on flocculation of fine particles. *Miner. Eng.* **2022**, *186*, 107745.
(41) Alarcón-Segovia, L. C.; Daza-Agudelo, J. I.; Rintoul, I. Multifactorial Effects of Gelling Conditions on Mechanical Properties of Skin-Like Gelatin Membranes Intended for In Vitro Experimentation and Artificial Skin Models. *Polymers* **2021**, *13*, 1991.
(42) Schirmer, M.; Jekle, M.; Becker, T. Starch gelatinization and its complexity for analysis. *Starch Staerke* **2015**, *67* (1−2), 30−41.
(43) Nguyen, T. Q.; Breitkopf, C. Determination of Diffusion Coefficients Using Impedance Spectroscopy Data. *J. Electrochem. Soc.* **2018**, *165* (14), No. E826.
(44) Yang, L.; Gan, L.; Zhang, Z.; Zhang, Z.; Yang, H.; Zhang, Y.; Wu, J. Insight into the Contact Impedance between the Electrode and the Skin Surface for Electrophysical Recordings. *ACS Omega* **2022**, *7* (16), 13906−13912.
(45) Khunti, K. Accurate interpretation of the 12-lead ECG electrode placement: A systematic review. *Health Educ. J.* **2014**, *73* (5), 610−623.
(46) Sazgar, M.; Young, M. G. Overview of EEG, Electrode Placement, and Montages. In *Absolute Epilepsy and EEG Rotation Review: Essentials for Trainees*; Sazgar, M., Young, M. G., Eds.; Springer International Publishing: Cham, 2019; pp 117−125.
(47) Abdullah, A. H. D.; Chalimah, S.; Primadona, I.; Hanantyo, M. H. G. Physical and chemical properties of corn, cassava, and potato starchs. *IOP Conf. Ser. Earth Environ. Sci.* **2018**, *160* (1), 012003.
(48) Chen, L.; Wang, J.; Huang, J.; Tu, T.; Li, L. Cost-trivial material contributes greatly: A review of the application of starch in energy storage systems. *J. Energy Storage* **2023**, *73*, 109060.
(49) Koduru, H. K.; Marinov, Y. G.; Scaramuzza, N. Review on Microstructural and Ion-conductivity Properties of Biodegradable Starch-Based Solid Polymer Electrolyte Membranes. *Starch Staerke* **2022**, *74* (1−2), 2100170.
(50) Koev, T. T.; Muñoz-García, J. C.; Iuga, D.; Khimyak, Y. Z.; Warren, F. J. Structural heterogeneities in starch hydrogels. *Carbohydr. Polym.* **2020**, *249*, 116834.
(51) Tananuwong, K.; Reid, D. S. DSC and NMR relaxation studies of starch−water interactions during gelatinization. *Carbohydr. Polym.* **2004**, *58* (3), 345−358.
(52) Liu, X.; Wang, Y.; Yu, L.; Tong, Z.; Chen, L.; Liu, H.; Li, X. Thermal degradation and stability of starch under different processing conditions. *Starch Staerke* **2013**, *65* (1−2), 48−60.
(53) He, H.; Li, Y.; Liu, H.; Kim, Y.; Yan, A.; Xu, L. Elastic, Conductive, and Mechanically Strong Hydrogels from Dual-Cross-Linked Aramid Nanofiber Composites. *ACS Appl. Mater. Interfaces* **2021**, *13* (6), 7539−7545.
(54) Hsieh, C.-F.; Liu, W.; Whaley, J. K.; Shi, Y.-C. Structure and functional properties of waxy starches. *Food Hydrocolloids* **2019**, *94*, 238−254.
(55) Hirankumar, G.; Mehta, N. Effect of incorporation of different plasticizers on structural and ion transport properties of PVA-LiClO4 based electrolytes. *Heliyon* **2018**, *4* (12), No. e00992.
(56) Lee, C.-J.; Wu, H.; Hu, Y.; Young, M.; Wang, H.; Lynch, D.; Xu, F.; Cong, H.; Cheng, G. Ionic Conductivity of Polyelectrolyte Hydrogels. *ACS Appl. Mater. Interfaces* **2018**, *10* (6), 5845−5852.
(57) Kotsialou, Z.; Makris, N.; Gall, S. Fundamentals of the electrocardiogram and common cardiac arrhythmias. *Anaesth. Intensive Care Med.* **2024**, *25* (3), 219−222.
(58) Lee, D.; Song, J.; Kim, J.; Lee, J.; Son, D.; Shin, M. Soft and Conductive Polyethylene Glycol Hydrogel Electrodes for Electrocardiogram Monitoring. *Gels* **2023**, *9* (12), 957.
(59) Tessier, A.; Zhuo, S.; Kabiri Ameri, S. Ultrasoft Long-Lasting Reusable Hydrogel-Based Sensor Patch for Biosignal Recording. *Biosensors* **2024**, *14* (8), 405.
(60) Liu, Q.; Zhou, J.; Yang, L.; Xie, J.; Guo, C.; Li, Z.; Qi, J.; Shi, S.; Zhang, Z.; Yang, H.; Hu, J.; Wu, J.; Zhang, Y. A reversible gel-free electrode for continuous noninvasive electrophysiological signal monitoring. *J. Mater. Chem. C* **2023**, *11* (26), 8866−8875.
(61) Halgren, M.; Ulbert, I.; Bastuji, H.; Fabó, D.; Erőss, L.; Rey, M.; Devinsky, O.; Doyle, W. K.; Mak-McCully, R.; Halgren, E.; Wittner, L.; Chauvel, P.; Heit, G.; Eskandar, E.; Mandell, A.; Cash, S. S. The generation and propagation of the human alpha rhythm. *Proc. Natl. Acad. Sci. U.S.A.* **2019**, *116* (47), 23772−23782.
(62) Zhu, H.; Cheng, C.; Yin, H.; Li, X.; Zuo, P.; Ding, J.; Lin, F.; Wang, J.; Zhou, B.; Li, Y.; Hu, S.; Xiong, Y.; Wang, B.; Wan, G.; Yang, X.; Yuan, Y. Automatic multilabel electrocardiogram diagnosis of heart rhythm or conduction abnormalities with deep learning: a cohort study. *Lancet Digital Health* **2020**, *2* (7), e348−e357.
(63) Conrardy, J.; Hillanbrand, M.; Myers, S.; Nussbaum, G. F. Reducing Medical Waste. *AORN J.* **2010**, *91* (6), 711−721.
(64) Fernandes, G.; Hassan, I.; Sridhar, D. Building resilient healthcare supply chains to manage pandemics in low- and middle-income countries. *Bull. World Health Organ.* **2022**, *100* (2), 174−176.

https://doi.org/10.1021/acssuschemeng.4c07823
ACS Sustainable Chem. Eng. 2025, 13, 6051−6063